ELSEVIER

Polymer 42 (2001) 1201–1206

polymer

www.elsevier.nl/locate/polymer

Dispersed structure change of smectic clay/poly(methyl methacrylate) nanocomposites by copolymerization with polar comonomers

M. Okamoto[a,*], S. Morita[a], Y.H. Kim[a], T. Kotaka[a], H. Tateyama[b]

[a]*Advanced Polymeric Materials Engineering, Graduate School of Engineering, Toyota Technological Institute, Hisakata 2-12-1, Tempaku, Nagoya 468-8511, Japan*

[b]*Inorganic Materials Department, Kyushu National Industrial Research Institute, Shuku-machi, Tosu-shi 841-0052, Japan*

Received 22 March 2000; received in revised form 22 May 2000; accepted 6 June 2000

Abstract

Via in situ free-radical copolymerization of methyl methacrylate (MMA) with a small amount of polar comonomers such as *N*,*N*-dimethylaminopropyl acrylamide (PAA), *N*,*N*-dimethylaminoethyl acrylate (AEA) and acrylamide (AA), we synthesized clay/copolymer-based nanocomposites from lipophilized smectic clay (SPN). The degree of dispersion and the intercalation spacing of these nanocomposites were investigated by using a transmission electron microscope (TEM) and X-ray diffraction (XRD), respectively. The introduction of the polar comonomers affected the features of both aggregation and flocculation (edge–edge) interactions. On incorporation of the PAA comonomer, a much stronger flocculation took place owing to the edge–edge interaction of the silicate layers. In contrast, the AA comonomer played an important role in delaminating the layers. Especially in the PMMA-AA (1 mol%)/SPN system, the ordered intercalated nanocomposite was formed as revealed by XRD and TEM. Each copolymer matrix nanocomposite showed a larger enhancement of moduli compared with the PMMA/SPN nanocomposite due to the large aspect ratio of the dispersed clay particles in the copolymer matrices.

Keywords: Nanocomposite; Polar comonomer; Edge–edge interaction

1. Introduction

In our previous paper [1], we synthesized clay/poly (methyl methacrylate) (PMMA) and clay/polystyrene (PS) nanocomposites via in situ intercalative polymerization using lipophilized smectic clays (called SPN and STN), which were modified by oligo(oxypropylene)-, diethyl-, methyl-ammonium cation and methyl-, trioctil-ammonium cation, respectively. Under some conditions, the intercalative nanocomposites, which were formed in both PMMA/STN and PS/SPN systems, exhibited flocculation [2] of clay particles because of the hydroxylated edge–edge interaction of the silicate layers. Further, for PMMA/STN and PMMA/SPN systems, the individual layers were stacked against each other and dispersed homogeneously in the PMMA matrix. The length of the oriented collections in the range of 100–300 nm is far larger than that in original clay (mean diameter $\cong$ 50 nm). Such flocculation and aggregation presumably are governed by an interfacial energy between the polymer matrix and clays and controlled by quarternized ammonium salt–matrix polymer interaction. The polarity of the matrix polymer is of fundamental importance in controlling the nanoscale structure.

In this paper, we report the results on the effect of copolymerization with a small amount of polar comonomers on the structure development of both flocculation and aggregation in a PMMA/SPN nanocomposite. We discuss the internal formed structure and mechanical properties of the nanocomposites.

2. Experimental

The organically modified smectic clay (SPN) used in this study, which was synthesized by an ion exchange reaction between Na^+-smectite and quaternized ammonium salt (QA), oligo(oxypropylene)-, diethyl-, methyl-ammonium chloride, $[(C_2H_5)_2(CH_3)N^+(O\text{-}iPr)_{25}]Cl^-$, was supplied by CO-OP Chemical Co. Ltd. The Na^+-smectite has an ion exchange capacity of 86.6 meq/100 g. Three polar comonomers, *N*,*N*-dimethylaminopropyl acrylamide (PAA; Kohjin Co. Ltd), *N*,*N*-dimethylaminoethyl acrylate (AEA; Kohjin Co. Ltd) and acrylamide (AA; Wako Pure Chemical Ltd,

* Corresponding author. Tel.: +81-52-809-1861; fax: +81-52-809-1864.
E-mail address: okamoto@toyota-ti.ac.jp (M. Okamoto).

0032-3861/01/$ - see front matter
PII: S0032-3861(00)00419-5

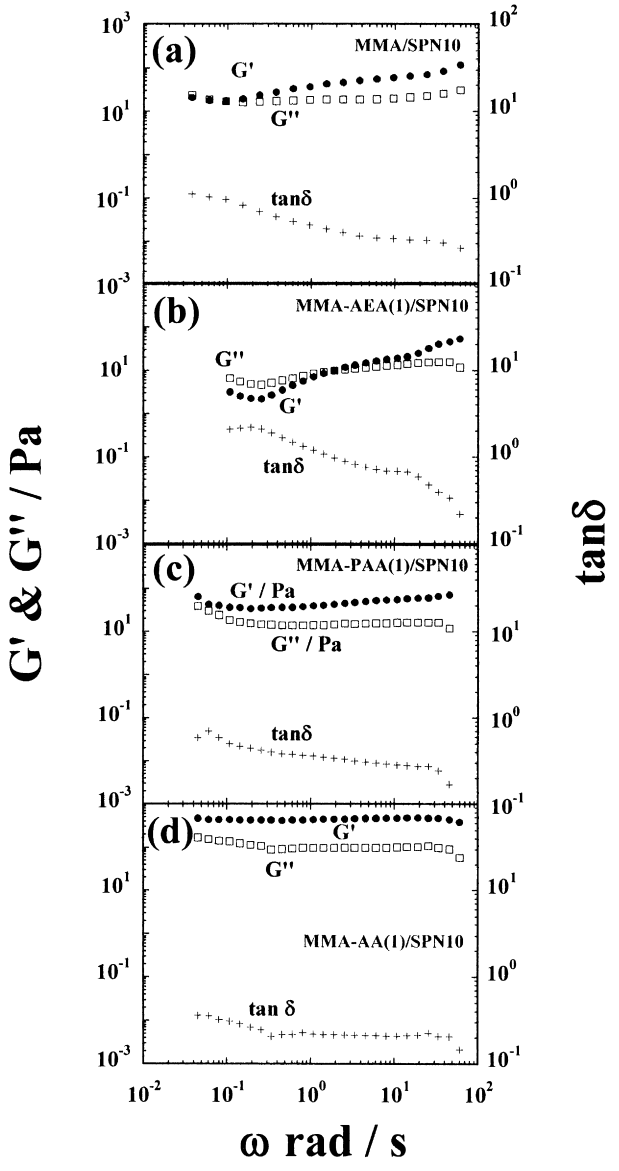

Fig. 1. Frequency ω response of the storage $G'(\omega)$, loss $G''(\omega)$ moduli and tan δ of: (a) MMA/STN10, (b) MMA-AEA (1 mol%)/SPN10, (c) MMA-PAA (1 mol%)/SPN10, and (d) MMA-AA (1 mol%)/SPN10 suspensions at 25°C.

GR) were used without further purification. The SPN solid was dispersed in MMA (Wako Pure Chemical Ltd, GR) including a small amount of the polar comonomer via ultrasonication (Ultrasonic 250, Hey Co.) at 25°C for 7 h to obtain suspensions. The details of the in situ intercalative polymerization were described elsewhere [1]. For comparison we prepared PMMA and a PMMA-based copolymer including QA as the references in the same manner. The structure analyses of X-ray diffraction (XRD) and transmission electron microscopy (TEM), and rheological properties of the suspensions and corresponding nanocomposites were carried out using the same apparatus as that described in the previous article [1].

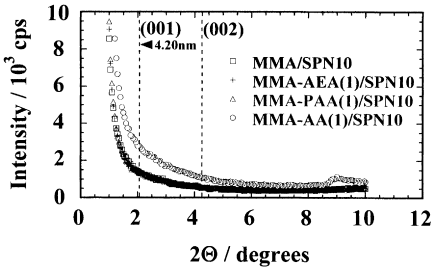

Fig. 2. X-ray diffraction patterns of suspensions. The dashed lines indicate the location of the silicate (001) and (002) reflections of solid SPN ($d_{(001)} = 4.20$ nm, $d_{(002)} = 2.02$ nm).

3. Results and discussion

3.1. Dispersed structure and dynamic viscoelasticity of suspensions

Fig. 1 shows the typical frequency ω dependence of storage $G'(\omega)$ and loss $G''(\omega)$ moduli for four different suspensions containing 10 wt% SPN in three different PMMA–comonomer mixtures within a range of linear viscoelasticity. The MMA/SPN10 suspension is a reference. Again, the code MMA-AEA(1)/SPN10 represents a suspension containing 10 wt% SPN in a 99/1 (mol rate) mixture of MMA and AEA. In the MMA/SPN suspension, we can clearly see that both moduli are dependent on ω, suggesting the system is a viscoelastic sol as shown in our previous paper [1]. Incorporation of only 1 mol% polar comonomer, however, alters the rheological behavior drastically depending on the type of comonomers in the system. For both MMA-AA(1)/SPN10 and MMA-PAA(1)/SPN10 systems, $G'(\omega)$ and $G''(\omega)$ are almost independent of ω and the value of $G'(\omega)$ is higher than $G''(\omega)$, which implies that these systems become a viscoelastic solid-like gel. On the other hand, in the MMA-AEA(1)/ SPN suspension, the stronger ω dependence of the moduli is observed as a typical sol system.

Fig. 2 shows a series of XRD patterns of the suspensions in the range of diffraction angle $2\Theta = 1$–$10°$. The mean interlayer spacing of the (001) plane ($d_{(001)}$) for the solid SPN obtained by XRD measurements is 4.20 nm [1], as indicated by the broken line in the figure. For each suspension, clearly the peaks arising from the (001) and (002) reflections of SPN disappear and the layer structure is destroyed. The absence of Bragg diffraction peaks indicates that the clay has been completely exfoliated or delaminated in the suspension. However, the complete exfoliation of the silicate layers is not judged from only these diffractograms.

In consideration of the results on the dynamic viscoelasticity and the corresponding XRD patterns for the viscoelastic solid-like suspension without structural regularity of silicate layers as discussed in our previous study [1], we may conclude that intercalated nanocomposites have been presumably formed, especially in the MMA-AA(1)/SPN10 system. In contrast, for the MMA-AEA(1)/SPN system, the

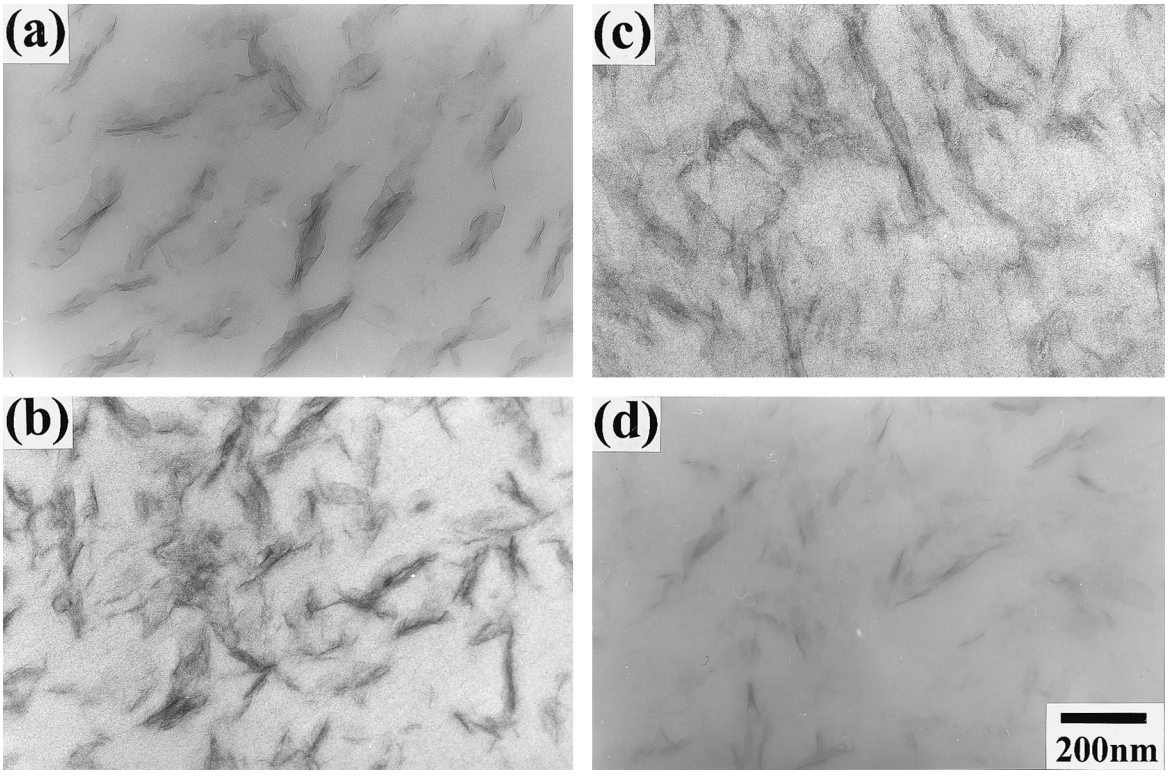

Fig. 3. TEM micrographs of a thin section of nanocomposites: (a) PMMA/SPN, (b) PMMA-AEA (1 mol%)/SPN, (c) PMMA-PAA (1 mol%)/SPN and (d) PMMA-AA (1 mol%)/SPN.

subsequent preparation of the nanocomposite leads to the flocculated structure due to the stacking of the silicate layers.

3.2. TEM observation and XRD patterns of copolymer-based nanocomposites

Figs. 3 and 4 show, respectively, the results of TEM bright field images and XRD patterns in the range of $2\Theta = 1$–10° corresponding to the nanocomposites shown in Fig. 2. As mentioned in our previous paper [1], in the PMMA/STN nanocomposite, the stacked silicate layers of about 200 nm length and about 40–50 nm thickness, which consist of about 10 parallel individual silicate layers, are observed randomly in the PMMA matrix but the coherent order of the silicate layers seems to be low. For MMA-AEA(1)/SPN10, the same behavior of the stacked silicate layers is observed but the thickness of the aggregation slightly decreases compared to that of PMMA/SPN10.

In the PMMA-PAA(1)/SPN nanocomposite, individual layers connected through the edge are seen in the PMMA-PAA(1) matrix and large anisotropy of the clay layers is observed. A much stronger flocculation takes place owing to the hydroxylated edge–edge interaction of silicate layers. In contrast, the PMMA-AA(1)/SPN10 nanocomposite exhibits less stacking of 4–5 layers with a distance of about 5 nm as a fine dispersion in the PMMA-AA(1) matrix. The coherent order of the silicate layers in this system is higher than that in other systems. The result is consistent with the XRD analysis. In the pattern of the PMMA-AA(1)/SPN nanocomposite, we see a small peak at $2\Theta = 3.50^\circ$ and a small remnant shoulder at $2\Theta \cong 5.27^\circ$ corresponding to the (002) and (003) planes, respectively. Unfortunately, we cannot follow the diffraction peak of the (001) plane because of the limitation of small-angle measurement. The calculated value of the basal spacing of the (001) plane ($d_{(001)}$) is $\cong 5.04$ nm ($2\Theta \cong 1.75^\circ$), which is larger than that of the original SPN solid. Presumably, the ordered intercalated nanocomposite has been formed during the polymerization.

The diffractograms of other nanocomposites show rather monotonously decreasing profiles with increasing 2Θ. As mentioned above, the coherent order of the silicate layers is lower compared to the PMMA-AA(1)/SPN10 nanocomposite.

Fig. 5 shows the results of TEM bright field images of PMMA-AA(3)/SPN and PMMA-AEA(3)/SPN nanocomposites, and in Fig. 6, we schematically summarize the dispersed morphology of clay layers in PMMA/SPN-based nanocomposites obtained from TEM pictures. The length versus thickness schemes of randomly dispersed silicate particles in the nanocomposites nicely demonstrates the characteristic effects of the polar group in each comonomer on the morphology. Incorporation of the 1 mol% AEA comonomer possessing a dimethyl amine group appears to lead to a slight edge–edge interaction. On the other hand,

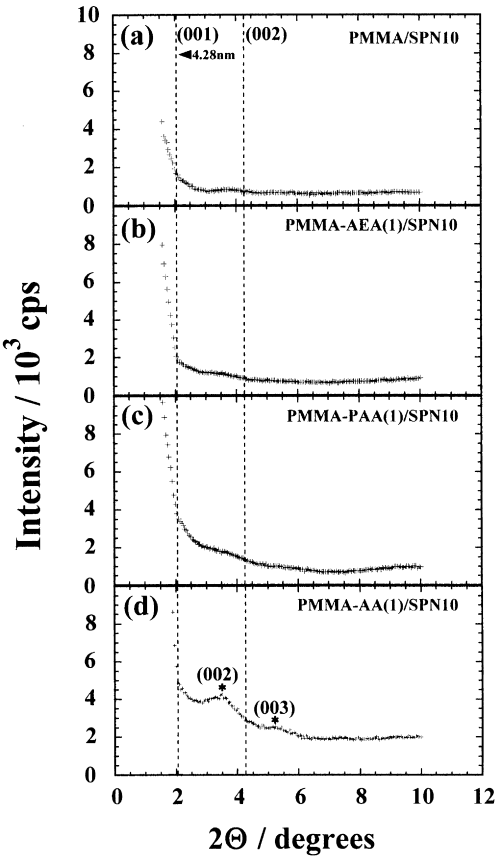

Fig. 4. X-ray diffraction patterns of the corresponding nanocomposites. The dashed lines indicate the location of the silicate (001) and (002) reflections of SPN solid ($d_{(001)} = 4.20$ nm, $d_{(002)} = 2.02$ nm). The asterisk in the panel (d) indicates the speculated position of (002) and (003) reflections of PMMA-AA (1 mol%)/SPN nanocomposite.

the introduction of the AA comonomer having an amide group appears to play an important role in delaminating the layers. However, in the case of the incorporation of 3 mol% AEA and AA, these polar comonomers lead to the stacking of the layers compared to the corresponding 1 mol% copolymer matrix systems due presumably to the strong hydrogen bonding between polar groups. For the PAA comonomer having both polar groups, a much stronger flocculation takes place owing to the edge–edge interaction of the layers.

Thus, owing to the interaction between clay layers and copolymer matrices with a small amount of polar groups, the dispersed morphology of the clay particles exhibits complex behavior. In other words, the introduction of the polar comonomers affects the features of both aggregation and flocculation (edge–edge) interactions. In recent years, Ginzburg et al. have analyzed the thermodynamics of disk-like particles dispersed in a polymer matrix using the Somoza–Tarazona free-energy function [3,4]. They pointed out that the disk–disk interaction plays an important role in determining the stability of clay particles and hence the morphology of such composites. Our morphology results are at least consistent with their prediction.

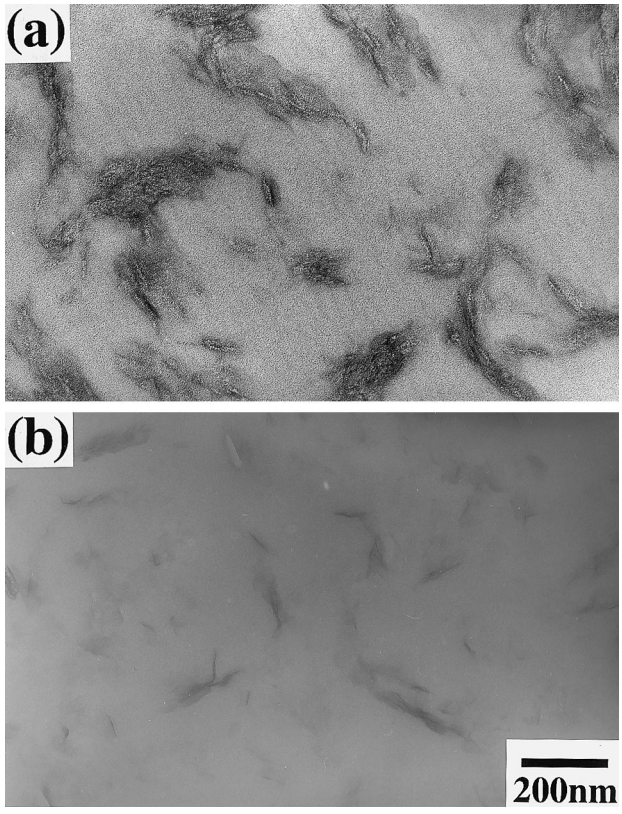

Fig. 5. TEM micrographs of a thin section of nanocomposites: (a) PMMA-AEA (3 mol%)/SPN, and (b) PMMA-AA (3 mol%)/SPN.

3.3. Mechanical properties and enhancement of modulus

Fig. 7 shows the temperature dependence of the isochronal modulus G' and loss tan δ of the copolymer-based nanocomposites and the corresponding clay-free copolymer/QA blends. For comparison, also shown are the data for PMMA/SPN10 and PMMA/QA (Fig. 7(a)). The data were taken at the frequency ω of 6.28 rad/s (= 1 Hz) with the amplitude γ of 0.05 and heating rate (dT/dt) of 2°C/min.

For PMMA/SPN10 and PMMA/QA blends, we see only a small difference between their G' and tan δ versus T curves

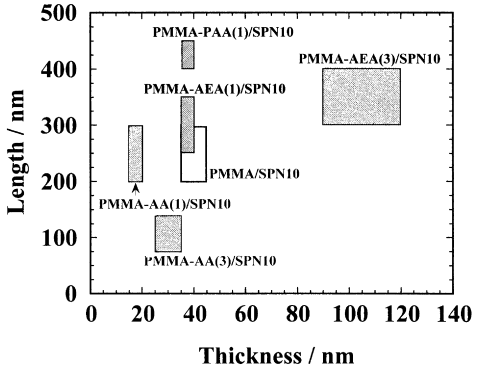

Fig. 6. Plots of length and thickness of the dispersed clay particles in various copolymer matrices estimated from TEM pictures. The estimated values are located within the shaded area.

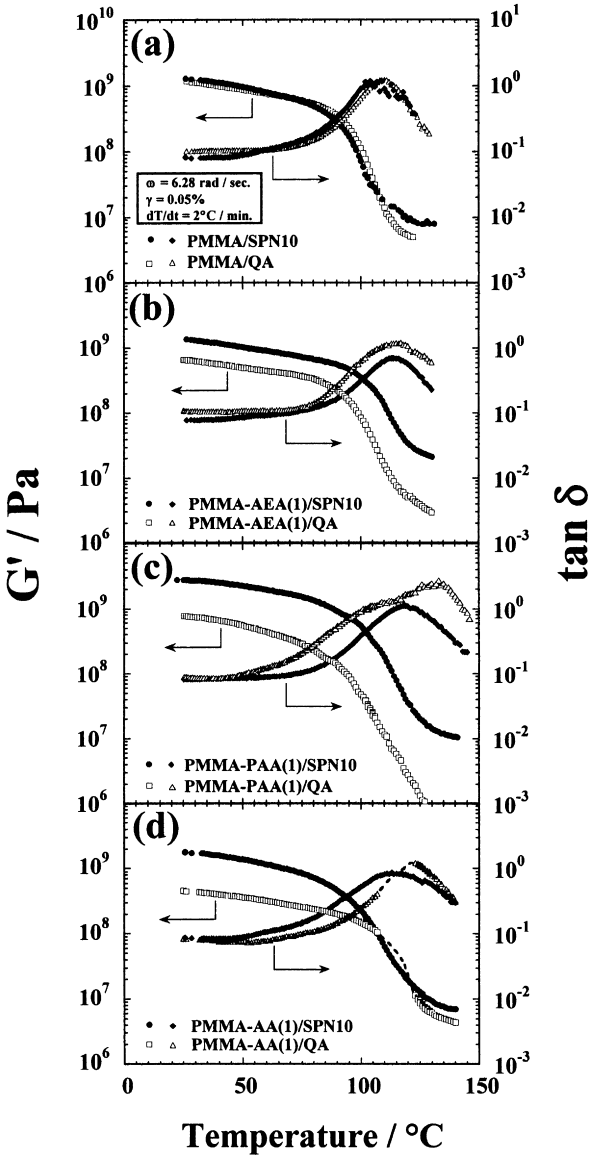

Fig. 7. Temperature dependence of G' and tan δ for the nanocomposites and polymerized copolymer/QA compositions without clays.

(Fig. 7(a)). The introduction of AEA, PAA and AA to PMMA as the copolymer matrix appears to suppress the decrease in G' with increasing temperature. In the glassy region below T_g, the G' of the copolymer-based composites are roughly 200–400% higher than those of the corresponding clay-free blends. We also notice that the tan δ peaks for the composites are somewhat lower and shifted to the lower-temperature side than those of the clay-free blends, especially for PMMA-PAA(1) and PMMA-AA(1) systems.

The behavior of PMMA-AA(1)/SPN10 is somewhat different from other systems. We see a broadening and a low-temperature shift of the tan δ peak and, nevertheless, the tan δ values above T_g are almost the same for the PMMA-AA(1) copolymer-based composite and the corresponding clay-free blend as shown in Fig. 7(d). The XRD pattern of the composite shown in Fig. 4(d) exhibits weak but significant reflection peaks from the expanded (002) and (003) planes. These results suggest that intercalation of the copolymer chains into the gallery of the clay layers has taken place, thus leading to the suppression of the mobility of the copolymer segments near the interface, which may be common for the polymer-based composite with reinforcing additives [5].

In Fig. 8, we summarized the clay content dependence of G' obtained at $\omega = 6.28$ rad/s and 30°C for seven different composites including randomly oriented glass-fiber- (GF-) reinforced PMMA (PMMA/GF). For comparison, here we show the previous data of PMMA/STN and PS/SPN nanocomposites [1]. The copolymer-based composites exhibit larger values of G'_{PCN}/G'_{matrix} compared with the PMMA/SPN nanocomposite. G'_{PCN} and G'_{matrix} are the moduli of the composites and the corresponding PMMA-copolymer/QA blend, respectively. The large reinforcement in the elastic modulus is observed in the figure. The essential factors governing the enhancement of mechanical properties is the aspect ratio of the dispersed filler particles. The Einstein coefficient k_E derived by Halpin and Tai's theoretical expression modified by Nielsen is shown in the figure [6]. Halpin and Tai's–Nielsen expression of the modulus of composite G'_{PCN} is given by:

$$\frac{G'_{PCN}}{G'_{matrix}} = \frac{1 + XY\phi_{filler}}{1 - Y\Psi\phi_{filler}} \tag{1}$$

where

$$X = k_E - 1 \tag{2}$$

$$Y = \frac{(G'_{filler}/G'_{matrix}) - 1}{(G'_{filler}/G'_{matrix}) + X} \tag{3}$$

$$\Psi = 1 + \left[\frac{1 - \phi_m}{\phi_m^2}\right]\phi_{filler} \tag{4}$$

Here, G'_{matrix} and G'_{filler} are the moduli of the matrix (i.e. PMMA/QA or PMMA) and fillers (clay or GF), respectively, X is a constant depending on the type of construction of composite materials and relates to the aspect ratio, k_E is the Einstein coefficient, and ϕ_{filler} and ϕ_m are the volume fraction of filler reinforcement and the maximum packing volume fraction of filler (0.63 for clay and 0.82 for GF [4]), respectively. Taking the modulus of the clay G'_{clay} to be 170 GPa [4] and that of GF to be 60 GPa [4], we calculated the composition dependence of G'_{PCN}/G'_{matrix} according to Eqs. (1)–(4) and the value of k_E was estimated by selecting an appropriate value for the best fit to the experimentally obtained G'_{PCN}/G'_{matrix} versus ϕ_{filler} plots. The results are summarized in Fig. 8.

The estimated value of k_E was 500 for PMMA-AA(1)/SPN, 160 for PMMA-PAA(1)/SPN, 60 for PMMA-AEA(1)/SPN, 30 for PS/SPN, 15 for PMMA/SPN, 7 for PMMA/STN nanocomposites and 7 for the PMMA/GF-reinforced material. The reason for the high modulus

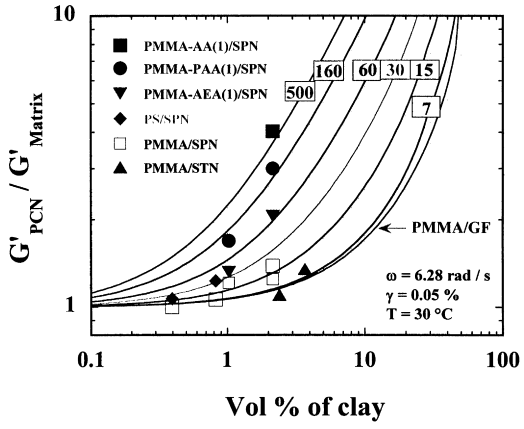

Fig. 8. Plots of G'_{PCN}/G'_{matrix} vs. volume% of filler for various nanocomposites. The Einstein coefficient k_E was shown with the number in the box. The lines show the calculated results from Halpin and Tai's theory with various k_E.

enhancement of the nanocomposites may be attributed to two factors: one is the larger k_E and the other is the higher value of G'_{clay} compared with that of GFRP.

The enhancement of the modulus explains the dispersed structure of clay in the nanocomposites reasonably well. The formation of the clay particles with the large aspect ratio is presumably due to the enhancement of interactions between clay layers and copolymer matrices with small amounts of the polar groups.

4. Conclusions

We demonstrated the effect of copolymerization with small amounts of polar comonomers on the structure development of both flocculation and aggregation (layer stacking) in a PMMA/SPN nanocomposite. Three polar comonomers, PAA, AEA and AA were selected. Incorporation of the AEA comonomer, possessing dimethyl amine group up to 3 mol%, leads to stacking of the layers. On the other hand, the introduction of an AA comonomer having an amide group plays an important role in delaminating the layers. For a PAA comonomer having both polar groups, the much stronger flocculation takes place owing to the edge–edge interaction of the layers. Both the aggregation and edge–edge interactions are altered due to the introduction of the polar comonomers. The copolymer matrix systems exhibit a larger enhancement of both storage and loss moduli compared with the PMMA/SPN nanocomposite due to the formation of the large aspect ratio of the clay particles with a small amount of the polar groups.

Acknowledgements

We would like to thank Dr Tuneo Chiba and Associate Prof. Toshiaki Ougizawa, Tokyo Institute of Technology for taking the TEM pictures shown in Figs. 3 and 5.

References

[1] Okamoto M, Morita S, Taguchi H, Kim YH, Kotaka T, Tatayama H. Polymer 2000;41:3887.
[2] Van Olphen H. An introduction to clay colloid chemistry. New York: Wiley, 1977.
[3] Ginzburg VV, Balazs AC. Macromolecules 1999;32:5681.
[4] Somoza AM, Tarazona P. J Chem Phys 1989;91:517.
[5] Nielsen LE. Mechanical properties of polymer and composites, vol. 2. New York: Marcel Dekker, 1981 (chap. 7, p. 233).
[6] Halpin JC, Kardos JL. Polym Eng Sci 1976;16:344.